Surfaces and Interfaces 30 (2022) 101880

Contents lists available at ScienceDirect

Surfaces and Interfaces

journal homepage: www.sciencedirect.com/journal/surfaces-and-interfaces

Malachite green removal using algal biochar and its composites with kombucha SCOBY: An integrated biosorption and phycoremediation approach

Abhijeet Pathy [a], Nageshwari Krishnamoorthy [a], Scott X. Chang [b], Balasubramanian Paramasivan [a,*]

[a] Department of Biotechnology and Medical Engineering, National Institute of Technology Rourkela, Odisha 769008, India
[b] Department of Renewable Resources, University of Alberta, Edmonton, Alberta T6G 2E3, Canada

ARTICLE INFO

Keywords:
Algae
Kombucha-SCOBY
Malachite green
Adsorption
Phycoremediation
Biochar

ABSTRACT

Malachite green pollution in the aquatic environment results in health hazards such as cancer and respiratory problems. Effective methods need to be developed to remove malachite green from wastewater. Here, we studied the adsorption of malachite green by a low-cost microalgal biochar (AB) and a novel microalgal-kombucha-SCOBY composite biochar (AKB). The maximum adsorption capacity of AB and AKB for malachite green was 166 and 500 mg g^{-1}, respectively. The kinetics and isotherm models indicate that chemisorption and diffusion were the dominant mechanisms driving the adsorption reactions. The partially remediated water from the adsorption experiment was phycoremediated to remove the remaining pollutants and to utilize the water for algal growth. Integration of phycoremediation with adsorption achieved removal efficiencies of >98% for both biochars. Moreover, microalgal growth was increased by 1.33 and 1.55 times in the AB and AKB remediated water, respectively, than in freshwater.

1. Introduction

Malachite green (MG, $C_{23}H_{25}C1N_2$) is an organic compound belonging to the class of triaryl methane dyes. Although malachite green has been banned in many developed countries, its illegal use is widespread in some countries due to its low cost and antimicrobial and dying properties [1]. Malachite green is, therefore, in demand in various sectors such as aquaculture, pharmaceuticals, fine chemicals, textiles, and food processing industries in some countries, leading to their production in tonnes on a global scale [2]. Malachite green's solubility and stability in water prevent its degradation by microbes, making it highly persistent. Despite MG's wide-ranging applications, their presence in water for a longer duration adversely affects the aquatic ecosystem. Moreover, its toxicity increases with its concentration, exposure time, and environmental temperature [3]. The direct/indirect exposure of humans to MG could result in mutagenesis, respiratory problems, carcinogenesis, and chromosomal fracture [4]. Hence, a sustainable approach that is facile and affordable is urgently needed for the remediation of MG in water bodies.

A variety of treatment methods, such as photocatalysis [5], microbial fuel cell [6], advanced oxidation [7], electrochemical oxidation [8] and adsorption [9], is available for removing malachite green from contaminated water. Among them, adsorption is one of the most effective and commonly implemented treatment techniques due to its simplicity and efficiency for contaminant removal. Several lignocellulosic [10,11] and carbonaceous materials (e.g., activated carbon) have been developed as adsorbents [12]. Apart from low cost biological materials, several porous nanostructures from polymers, clays, nanomaterials, and magnetic materials were developed for MG removal [13]. However, the search for cheaper adsorbents with high adsorption and regeneration capacities motivates new research. In past years, the introduction of biochar as an adsorbent has helped overcome some of the limitations (cost and ease of production) of activated carbon. However, not all biochars are effective for wastewater treatment. Therefore, chemical and physical modifications have been developed to enhance the properties of biochars for wastewater remediation [14]. It is evident that the pre-and post-treatment/activation of biochar helps achieve desirable characteristics of biochar; yet, it makes the production

* Corresponding author.
E-mail address: biobala@nitrkl.ac.in (B. Paramasivan).

https://doi.org/10.1016/j.surfin.2022.101880
Received 15 November 2021; Received in revised form 13 February 2022; Accepted 12 March 2022
Available online 14 March 2022

process more challenging from an economic and environmental perspective. The chemical activation of biochar generally involves using a significant amount of acids, alkali, or metal oxides, which is chemical-intensive and poses questions regarding its environmental sustainability [15]. On the other hand, physical activation does not require chemicals; but the necessity of higher temperature and other conditions makes the process energy- and cost-intensive.

This study had attempted a modification method that could balance the trade-off existing between chemical-intensive activation methods and the energy- and cost-intensive nature of physical activation methods without compromising the quality of biochar. It is a well-established fact that biomass's choice affects the biochar's physicochemical properties. Hence, careful consideration was given while choosing the biomass for biochar production. With the development of algal biorefinery approaches in recent years, the production and utilization of algal residues are becoming an issue. Converting algal residues to value-added products such as biochar will help us manage the huge amount of waste generated by algal industries and serve in several environmental applications [16]. In the past several years, an increasing amount of research has focused on algal biochar's properties and applications. Algal biochar is different from biochars produced from conventional biomass. Algal biochar generally has a lower surface area and carbon content; however, the presence of a large number of functional groups makes it an efficient adsorbent [17]. Thus, in this study, the objective is to prepare biochars from algal biomass and then undertake novel modification to improve the synthesized adsorbent's characteristics. In recent years, composites of biochar have been prepared by modifying biochars with different substances such as clay [18], metals (by forming layered double hydroxide) [19], polymers (such as chitosan) [20] for using it as an adsorbent. Hence, the biochar was modified with a natural polymer (cellulose) in this study. Kombucha SCOBY (symbiotic culture of bacteria and yeast) is a cellulose byproduct of kombucha fermentation. The SCOBY generated has several applications in the food and health sector; however, it gets discarded due to contamination and unexplored applications [21]. Still, the cellulose sheets can be thermochemically converted into value-added products such as biochar. Moreover, the SCOBY is primarily made up of cellulose, and hence it can be utilized to modify certain aspects of algal biomass while producing biochar. It has been hypothesized that adding SCOBY to algal biomass might enhance the surface area while retaining the surface functional groups of algae.

Most previous adsorption experiments have been focused on remediating the polluted water but do not discuss or demonstrate the fate of the remediated water [3,22]. However, the utilization of the remediated water is equally essential, as its remediation is a research gap in adsorptions studies. Priyan et al [23] discussed the ecotoxicological assessment of diclofenac by utilizing the remediated water for growing plants, microbes, and fish. Thus, the fate and use of remediated water need to be discussed in studies to encourage their use in different activities. Hence, in this study, we used biochar-remediated water to cultivate microalgae to address this research gap. This approach served two purposes: (1) it helps in remediating the remaining MG after the adsorption process, (2) using the remediated water for algal growth consequently reduces the dependence on freshwater. This makes the process cyclical and sustainably plausible and encourages the research and industrial communities to tap the potential of the post adsorption process.

This study produced biochars from kombucha SCOBY, microalgal biomass, and composite for removing malachite green from an aqueous solution. The objectives were to (1) characterize the prepared biochars for comprehending the properties required for adsorption, (2) optimize the batch experimental conditions (contact time, pH, biochar dosage, initial concentrations of MG, and presence of an acidic dye) for remediating malachite green, (3) understand the mechanisms of malachite green removal by fitting various kinetics and isotherm models, (4) integrate phycoremediation process for completely remediating malachite green from water and utilizing the remediated water for cultivating algae. Moreover, desorption and regeneration studies were carried out for five consecutive cycles to validate the reusability of the prepared adsorbents.

2. Materials and methods

2.1. Microalgal cultivation and kombucha SCOBY production

The microalgal samples were collected from the Naga pond at National Institute of Technology (NIT) Rourkela (22.2604° N, 84.8536° E). *Chlorella sp., Scenedesmus sp., Synechocystis sp., and Spirulina sp.* were the dominant strains [24]. The mixed consortium was acclimatized in 6.5% of human urine and cultured in a photobioreactor under controlled temperature (25 ± 3 °C), and light intensity (natural solar radiation 100–900 W m^{-2}). The photo and dark periods were maintained at a 14:10 h ratio. Once the algal growth reached the stable phase, the biomass was harvested by chemical flocculation using ammonium chloride.

Tea waste was collected from a black and green tea processing plant (Parry Agro-House of Tea) located in Valparai, Tamil Nadu, India. The starter culture and SCOBY were collected from the Food Microbiology lab of the Department of Life Science, NIT Rourkela, and were maintained in a sugared (sucrose, $C_{12}H_{22}O_{11}$) waste black tea medium. The tea waste and sugar concentrations were 80 and 12 g L^{-1}, respectively. The mixture was boiled until the extract completely seeped into the medium and then allowed to cool. Later, the sample was inoculated with 5% kombucha broth and 5% SCOBY and incubated at room temperature for two weeks with an inherent pH of 4.5 ± 0.1.

Kombucha was made of several organic acids, minerals, vitamins, and anions, whereas the SCOBY was mainly cellulose and water. The composition of the used kombucha broth and SCOBY, along with their detailed preparation methods, can be found in Jayabalan et al [25]. The SCOBY cellulose sheets formed on the surface as a byproduct were used for pyrolysis.

2.2. Production of biochars

The harvested microalgal biomass was dried at 40 ± 3 °C for 48 h. The kombucha SCOBY cellulose was collected and stored as-is. Then the dried algal biomass and SCOBY were mixed in a 1:2 w:w ratio. The mixture was ground using a household grinder and stored at room temperature (27 ± 3 °C) for 8 h. Then it was loaded in a 500 mL stainless steel container in such a way that the biomass mixture filled 80–90% of the container, which was further sealed with aluminum foil and tightly closed. The steel container was then placed inside a top-lift muffle furnace. Similarly, the dried algal biomass and wet kombucha cellulose were separately packed with minimum headspace and placed inside the muffle furnace. The biomasses were pyrolyzed at 500 °C for a period of 45 min with a heating rate of 5 °C min^{-1}. Then the samples were allowed to cool down to room temperature and labeled as AB, KB, and AKB for algal biochar, kombucha SCOBY biochar, and algal-kombucha biochar, respectively.

2.3. Material characterization

The functional groups present in the biochar samples were analyzed through Fourier Transform Infrared Spectroscopy (FTIR) (Alpha ATR-FTIR, Bruker). The X-Ray Diffraction (XRD) analysis was performed with a 40kV, 40 mA and 3 kW diffractometer equipped with Cobalt-Iron radiation (Bruker AXS D8, Advance with Davinci Design). The surface morphology of the samples was analyzed using Scanning Electron Microscopy (SEM) (JEOL JSM- 6480 LV, EDS: Oxford Instruments). The elementary composition of the biochar was obtained by Energy-dispersive X-ray spectroscopy (SEM-EDS). A BET surface analyzer (Quantachrome/ AUTOSORB-1) used the N_2 adsorption/desorption

process to assess the surface properties such as pore size, pore volume, and surface area. The pH and conductivity of the biochar samples were measured using a multiparameter water quality meter (Labman Scientific Instruments, model- LMMP-3).

2.4. Adsorption experiments

Malachite green (analytical grade) procured from Himedia Corporation, India, was used for all experiments. The batch adsorption experiments were carried out in a 100 mL conical flask at room temperature (27 ± 3 °C). In each conical flask, 0.05 g of biochar was added to 50 mL of a 100 mg L^{-1} malachite green. The solution was stirred for 8 h at 150 rpm. To understand the influence of pH, the pH of the MG solution was varied (2–7) before the experiment by using 0.1 M NaOH/HCl. Then, to find the optimum adsorbent dosage, experiments were performed by varying the biochar concentration between 0.5–1.5 mg mL^{-1}. The MG concentration was varied from 20 to 200 mg L^{-1} to check the effect of initial MG concentration on adsorption efficiency. The effect of the presence of acidic dye was investigated by mixing different concentrations of MG and methyl orange (MO). An adsorbent is evaluated based on its reusability (the number of cycles it can be reutilized). It is also essential to desorb the MG and convert it into solid crystals for reuse. Ethanol was used as the desorbing solvent to carry out the desorption experiments. For finding an optimum ethanol concentration, the desorption experiment was conducted by mixing different proportions of ethanol and water (1:0, 3:2, 1:1, 2:3, and 0:1).

The MG concentration was measured at 617 nm using Go Direct® SpectroVis® Plus Spectrophotometer (Vernier, USA). All the experiments were carried out in triplicates. The removal efficiency (*E%*) and adsorption capacity (q_e) of the biochars were estimated using Eqs. (1) and (2):

$$\text{Adsorption Capacity} = \left(\frac{C_i - C_e}{W}\right) \times V \quad (1)$$

$$\text{Removal Efficiency} = \left(\frac{C_i - C_e}{C_i}\right) \times 100 \quad (2)$$

where C_i and C_e are the initial and equilibrium concentration of MG in the solution (ppm), W is the weight of biochar added (g), and V is the total volume of the solution used in the adsorption experiment (mL).

2.5. Isotherms and kinetics

Assessment of the MG adsorption on AB and AKB biochar for understanding its sorption mechanism was performed using different kinetics and isotherm models. The details of isotherm and kinetic models implemented in this study are in the supplementary materials (Tables S1 and S2).

2.6. Phytoremediation and algal cultivation using remediated water

The adsorption experiments (with a reaction volume of 500 mL) were carried out under the optimized experimental conditions (obtained from the batch experiment) in a 1 L conical flask. The conical flasks were stirred with a magnetic stirrer for 5 h. Then the solution was allowed to settle (for approximately 30–45 min), and the supernatant (remediated water) was collected. 300 mL of remediated water obtained from AB and AKB adsorption experiment was added in 500 mL conical flasks and labeled as ABR (algal biochar remediated) and AKBR (algal kombucha biochar remediated) water, respectively. Along with these, one positive control (fresh distilled water) and one negative control (100 mg L^{-1} MG solution) were also prepared. For microalgae cultivation, one of the most common algal growth media (BG-11) was used; more specifically, 0.492 g of BG-11 media (Himedia, M1514) was added to all flasks containing 300 mL solution as per the standard protocol.

Microalgal inoculums (10% by volume) were then added to the remediated water samples and allowed to grow under controlled temperature (25 ± 3 °C) and light intensity (205 μmol photons m^{-2} sec^{-1}). The photo and dark periods were maintained at a 14:10 h ratio. The algae were allowed to grow for ten days. And the liquid samples were collected daily (till the maximum adsorption capacity was reached) to investigate the effectiveness of the phycoremediation process. Then on day 11, the algae was harvested (by centrifugation), dried, and weighed. The algal productivity was calculated using Eq. (3).

$$\text{Algal productivity} = \frac{\text{Final weight of algal biomass } (mg) - \text{ Initial weight of algal biomass } (mg)}{\text{Total days of cultivation } (day)} \quad (3)$$

3. Results and discussion

3.1. Physicochemical properties of biochars were affected by feedstock type

The elementary composition of used biomass and their respective biochars were evaluated (Table S3). The KB had the highest amount of carbon content (80%); however, the elemental composition of AB and AKB indicates the presence of inorganic compounds of significant nutritional value. The characterization details of the adsorbent are given below.

FTIR analysis indicates the presence of a diverse set of functional groups in both the AB and AKB samples (Fig. S1). The distinct peaks of functional groups can be seen to be present in the pyrolyzed algal biochar sample at 1028 cm^{-1}, 1622 $cm^{-1,}$ and 3268–3500 cm^{-1}, corresponding to S=O, C=C, and O-H stretches, respectively. In the case of kombucha SCOBY and kombucha SCOBY biochar, a strong and broad O-H stretch was present. Also, with an increase in temperature while charring, the C=C bonds present in kombucha SCOBY biomass were lost, which can be correlated with the low adsorption capacity of kombucha biochar. In AKB, significant peaks were located at 1018 cm^{-1} (S=O), 1634 cm^{-1} (C=C) and 3363 cm^{-1} (O-H). The AKB had transmittance even lower than AB for all major peaks (C=C, S=O, O-H) (Fig. S1), indicating higher bonds in AB. The reduced amount of functional groups in AKB could be attributed to the reduced fraction of microalgae in the algal composite biomass and biochar. The oxygen-containing groups, aromatic/phenolic groups, hydroxyl, and carboxyl groups present on the exterior of biochar can play a crucial role in the adsorption of pollutants [26]. For instance, anionic carboxylic groups help bind with a cationic dye such as MG; OH groups could help form the coordinate bonds with MG [27]. This is following the removal efficiency of AB and AKB, where the efficiency was greater with AB during the initial hours compared to AKB (Fig. 1a). The adsorption could be of two forms: chemical and physical. Chemical adsorption or chemisorption occurs when a chemical bond is formed between the adsorbate molecule (MG) and the functional groups on the adsorbent surface (biochar). Physical adsorption depends on physical forces such as van der Waals forces. Hence, having a larger

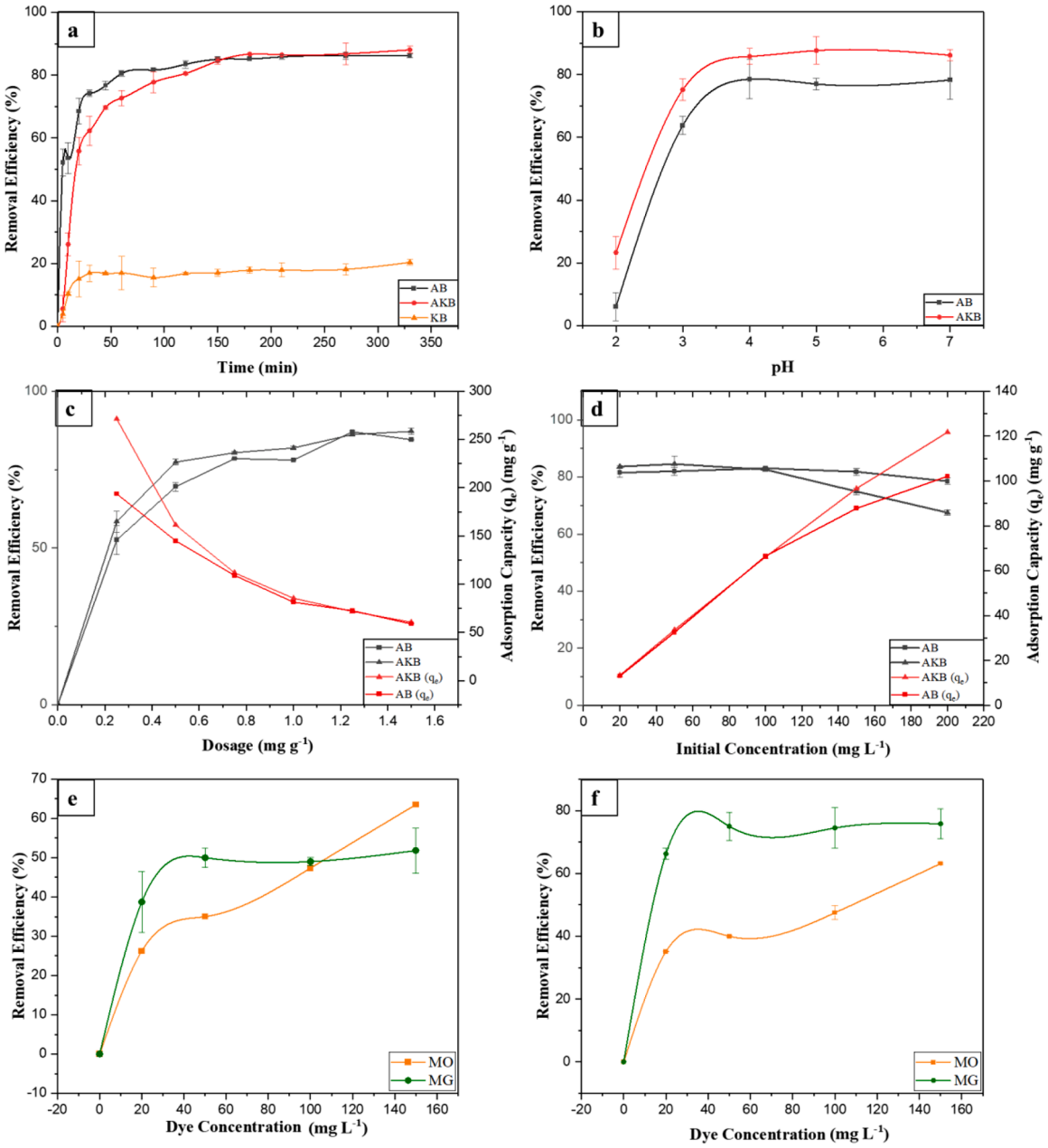

Fig. 1. Effect of experimental parameters on malachite green removal (a) Time; (b) pH; (c) Initial concentration of malachite green in the solution; (d) Dosage of biochar in the solution; Effect of methyl orange dye on adsorption of malachite green by (e) Algal biochar; (f) Algal kombucha biochar.
q_e: Amount of compound adsorbed at equilibrium (mg g^{-1}), AB: Algal biochar, AKB: Algal kombucha biochar, MG: Malachite green, MO: Methyl orange.

surface area could accommodate many adsorbate molecules through physical interactions. Moreover, a porous structure enables the adsorbate to diffuse into it. Though the adsorption capacity of AB was higher at initial levels, after a certain period of time, it could be possible that chemisorption was taken over by diffusion into pores. This is because the AB has a comparatively greater abundance of functional groups (as evident from FTIR analysis) than AKB. In contrast, the latter has a higher surface area and pore volume than AB. Thus, the greater abundance of functional groups might have played a crucial role in chemisorption, whereas the diffusion was facilitated by surface area and pore volume.

The XRD plots (Fig. S2) for biochar samples revealed distinct peaks at 2Θ of 32.5, 53.5, and 58.9° for AB, which can be due to the presence of carbon oxide (JCPDS No. 76-2378), calcium oxide silicate chloride (JCPDS No. 43-0086). In the case of KB, the XRD graph exhibited amorphous characteristics. The crystalline cellulose structures of SCOBY cellulose could have been lost due to the breakdown during biomass conversion via pyrolysis. However, with algal biochar modified with cellulose (AKB), additional peaks at 2Θ of 30.0, 31.1, 34.6, and 37.2° were observed. The distinct sharp peaks present in AB and AKB indicate the crystalline structure, whereas the broad peak in KB represents the amorphous nature of kombucha biochar. The 2Θ peaks in between 26 and 33° correspond to disordered (002) graphite planes in both AB and AKB [28]. AKB had a higher number of asymmetric reflexes than AB, showing more disorderliness in the structure. It could be due to the presence of two different materials in the biochar composite.

SEM analysis shows the surface properties of the prepared biochars (Fig. S3). It can be observed that the algal biochar and AKB had a large surface area and microporous structure suitable for and diffusion. The EDS analysis of the sample shows the carbon weight fraction of AB, KB, and AKB to be 40.7, 75.9, and 58.9%, respectively (Fig. S3). The AB and

AKB contained diverse elements, including silicon, chlorine, iron, aluminum, calcium, magnesium, and phosphorus, which may have contributed to the formation of enormous O-containing groups on the surface responsible for adsorption. In KB, most of the weight percentages were contributed by carbon and oxygen. However, morphological and anatomical changes occurred due to the modification of algal biomass with SCOBY cellulose. The latter contributed to the large surface area, and the former contributed to the surface functional groups, resulting in AKB having better adsorption characteristics.

From the BET analysis of the prepared biochars, the specific surface area (SSA) of AB, KB, and AKB were 2.98, 6.53, and 7.52 $m^2\ g^{-1}$, respectively. Biochars derived from algal biomasses have been reported to have a lower surface area. On the other hand, kombucha SCOBY is a porous, lightweight material with cellulose nanofibrils arranged as a three-dimensional network [29]. Hence, when the biochar was produced from the composite of algae and kombucha, the surface area increased from 2.98 to 7.52 $m^2\ g^{-1}$. For most biochar samples, the SSA was in the range of 0.9–28.50 $m^2\ g^{-1}$ [30]. The pore diameter for the biochar was in the range of 3.12–3.5 nm, which indicates that the biochars are mesoporous. The micropore volume of AB, KB, and AKB are 0.031, 0.084, and 0.065 $cm^3\ g^{-1}$, respectively.

3.2. Process conditions affected MG removal using biochar

3.2.1. Effect of contact time

For AB, 80% of the MG was removed in the first 60 min of the adsorption process, whereas for AKB, the removal efficiency was 70% in the 1st hour (the rapid adsorption phase) (Fig. 1a). Then the slower adsorption phase started, and the removal efficiency of AB (from 80 to 85%) and AKB (from 70 to 88%) steadily reached equilibrium in 180 min. However, KB reached equilibrium in the 1st hour, as KB had a poor affinity towards MG adsorption (removal efficiency was around 20%). This could be due to the absence of adsorption sites on KB surface. The rapid adsorption rate could be due to the availability of a higher number of active adsorption sites and surface pores on the biochar. But with the advancement of the adsorption process, the MG molecules started building up on the surface, and this build-up hinders the diffusion into the pores resulting in slower adsorption [31].

3.2.2. Effect of pH

The role of pH in the adsorption process is paramount as it affects the chemical characteristics of both the adsorbent and the adsorbate, the dissociation of functional groups on the active sites of the biochar, and the ionization of the substance in the solution. The solution pH affected the adsorption of MG (Fig. 1b). With the increase in pH from 2 to 4, the removal efficiency of AB and AKB reached 88 and 78%, respectively, representing an increase of 60% for both biochars. The removal efficiency remains unaltered from pH 4–7. Similar trends for MG adsorption have been reported previously by Chowdhury et al [32]. As a cationic dye, the MG exists as positive ions in aqueous solutions. In a highly acidic environment, the functional groups on biochar surfaces were protonated and positively charged, restricting the adsorption of positively charged MG ions onto the biochar surface. Moreover, H^+ as a positively charged ion could also compete with the MG cations for the limited active sites on the adsorbent's surface. Therefore, biochar adsorption of MG is not effective in highly acidic pH, but the adsorption efficiency increases with increasing pH.

3.2.3. Effect of dosage and initial ion concentration

The removal efficiency for AB (from 50 to 80%) and AKB (55 to 88%) increased with an increase in biochar dosage (Fig. 1c); this could be due to the greater availability of the active adsorption sites. However, the adsorption capacity decreased with the increase in dosage. This can be attributed to the aggregation of the adsorbent particles at a higher concentration [33]. The adsorption capacity increased for both AB (from 13 to 103 mg g^{-1}) and AKB (from 13.4 to 123 mg g^{-1}) with the increase in MG concentration from 20 to 200 mg L^{-1} (Fig. 1d). The increase in MG concentration might have accelerated the diffusion of MG particles from the bulk solution to the surface of the biochar, facilitating more adsorption reactions and increasing the adsorption capacity. However, on the contrary, with the increase in MG concentration, the removal efficiency for AB and AKB decreased by 10% (from 81.5 to 73%) and 5% (84.5 to 78%), respectively, due to the adsorbent having limited active sites available for adsorption; thus, after the saturation of these active sites, the adsorption decreases [34].

All the above reactions have been carried out at room temperature (27 ± 3 °C); the intention is to make the process affordable and least energy-intensive so that the results obtained from this study could be employed at a larger scale in an economical manner.

3.3. Isotherm of MG adsorption on biochar governed by its surface properties

Out of the eight models investigated for the adsorption behavior of AB and AKB for MG removal, three models showed a better fit with a strong r^2 value (Fig. 2a–c). Among them, the adsorption of MG dye onto AB biochar fitted very well to Freundlich ($r^2 = 0.99$) and Halsey ($r^2 = 0.99$) compared to the Langmuir model ($r^2 = 0.96$) (Table 1). In the case of AKB, the correlation coefficient for Freundlich, Halsey, and Langmuir models were 0.99, 0.99, and 0.98, respectively.

From the Langmuir model, the maximum monolayer adsorption capacity for AB and AKB was 166 and 500 mg g^{-1}, respectively. Moreover, the separation factor (R_L) can be used to examine the favourability of the adsorption process. The adsorption process is favorable if $0 < R_L < 1$. The R_L values for AB and AKB were between 0 and 1. Hence, it can be concluded that the adsorption process of MG into AB and AKB is favorable. Similarly, the Freundlich parameter (n_f) also provides an idea about the feasibility of the sorption process; n_f value more than one favors adsorption. In this study, the n_f for Mg adsorption AB and AKB were 1.85 and 1.47, respectively. This is aligned with Langmuir indicates the favorability of the adsorption process. Further, the accurately fitting data with Freundlich and Halsey isotherm suggest that the adsorption of MG on both biochars (AB and AKB) was multilayer adsorption, and the adsorbed molecules on the surface can interact with each other [35]. It also confirms that the prepared biochar has heterogeneous adsorption sites [36]. Moreover, fitting with Halsey isotherm indicates that adsorption has a uniform energy distribution [11].

3.4. Physicochemical properties of biochars influenced the kinetics and mechanism of MG adsorption on biochar

The MG adsorption on AB and AKB biochar are best fitted with pseudo-second-order kinetics (Table 2) compared to the pseudo-first-order kinetics (Fig. S4). Moreover, the plots showed good linearity with the Elovich model, implying that MG adsorption also follows the Elovich (Fig. 3). The pseudo-second-order model describes the sharing and exchanging of electrons between the adsorbent and the adsorbate; the primary forces associated with these types of interactions are covalent forces and ion exchange reactions. In contrast, the Elovich model elucidates the chemisorption kinetics of a heterogeneous surface adsorbent [37]. As the adsorption of MG on both biochars fitted well with both the pseudo-second-order and Elovich models, it can be concluded that MG adsorption was dominated by chemisorption on a heterogenous biochar surface.

The intraparticle diffusion (IPD) and diffusion-chemisorption models were also fitted to understand the process further and determine the rate-controlling steps. The IPD model assumes that intraparticle diffusion exclusively controls adsorption [38]. The fit exhibits non-linear plots and low R^2 values (Table 2), indicating the involvement of multiple steps in the adsorption process. The overall IPD can be separated into three distinct stages, with the magnitude of the rate constants (slopes) in the order of $K_1 > K_2 > K_3$ (Fig. S5). Possible explanations for

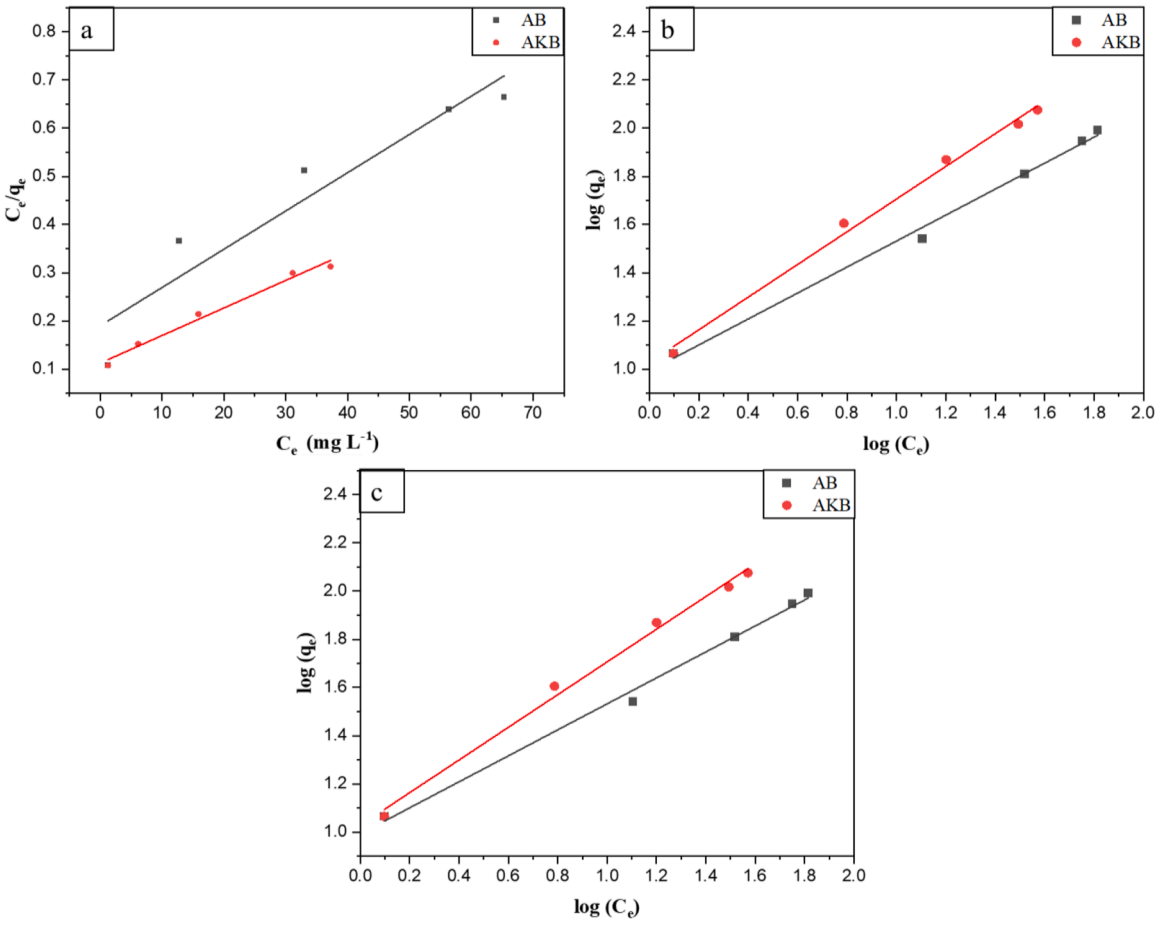

Fig. 2. Isotherms fitted for malachite green adsorption by algal biochar and algal kombucha biochar; (a) Langmuir; (b) Fruendlich; (c) Halsey.
C_e: Equilibrium concentration of adsorbate (mg L^{-1}), q_e: Amount of compound adsorbed at equilibrium (mg g^{-1}), AB: Algal biochar, AKB: Algal kombucha biochar

Table 1
Fitting results of adsorption isotherm models for MG removal using biochars.

Isotherm models	AB Model parameters	Correlation coefficient (r^2)	Adj. r^2	*p*-value	RMSE	AKB Model parameters	Correlation coefficient (r^2)	Adj. r^2	*p*-value	RMSE
Langmuir	q_m = 166.66 K_l = 0.0066	0.905	0.874	0.01	0.081	q_m = 500 K_l = 0.0025	0.983	0.978	$8.74*10^{-4}$	$1.31*10^{-2}$
Frendulich	n = 1.85 K_f = 9.81	0.994	0.992	$1.68*10^{-4}$	0.032	n = 1.47 K_f = 10.64	0.993	0.991	$2.21*10^{-4}$	0.038
D-R	β = -0.80 Q_m = 67.15	0.799	0.733	0.04	0.453	β = -0.90 Q_m = 81.94	0.849	0.799	0.02	0.424
Halsey	n_H = -1.85 K_H = 0.79	0.994	0.992	$1.68*10^{-4}$	0.032	n_H = -1.47 K_H = 0.75	0.993	0.991	$2.21*10^{-4}$	0.038
Kiselev	K_i = -24.73 K_n = -1.50	0.814	0.752	0.03	2.822	K_i = -60.98 K_n = -1.22	0.720	0.626	0.06	3.371
Flory-higgins	n = -1.329 K_{fh} = 0.05	0.841	0.789	0.02	0.214	n = -2.007 K_{fh} = 0.02	0.942	0.923	0.005	0.118
Temkin	b = 119.68 K_t = 0.93	0.887	0.849	0.01	14.054	b = 81.18 K_t = 0.88	0.949	0.933	0.004	11.455
Jovanovic	K_f = 0.023 Q_m = 11.69	0.854	0.806	0.02	0.386	K_f = 0.02 Q_m = 12.78	0.786	0.715	0.04	0.506

AB: Algal Biochar, AKB: Algal Kombucha Biochar; MG: Malachite green; D-R: Dubinin–Radushkevich; q_e – Adsorbate adsorbed per gram of the adsorbent at equilibrium (mg g^{-1}); q_m – Monolayer coverage capacity (mg g^{-1}); K_l – Langmuir isotherm constant (L mg^{-1}); C_e – Equilibrium concentration of adsorbate (mg L^{-1}); K_f – Freundlich isotherm constant ($mg^{1-(1/n)}$ $L^{1/n}$ g^{-1}); n – adsorption intensity; K– Dubinin–Radushkevich isotherm constant related to the adsorption energy (mol ^{2}); Q_m – theoretical isotherm saturation capacity (mg g^{-1}); K_H – Halsey isotherm constant; n_H – Halsey equation exponents; K_i – Kiselev equilibrium constant (L mg^{-1}); K_n – constant of complex formation between adsorbed molecules; K_{FH} – Flory–Huggins equilibrium constant (L mg^{-1}); n_{FH} – model exponent; K_T – Temkin isotherm equilibrium binding constant (L mg^{-1}); B_T- Temkin isotherm constant; K_J – Jovanovic isotherm constant (L mg^{-1}); q_{max} – maximum adsorption capacity in Jovanovic model (mg g^{-1}), Adj. r^2: Adjacent r^2, RMSE: Root mean square error.

Table 2
Fitting results of adsorption kinetic models for MG removal using biochars.

Model	MG Concentration (mg/L)	AB Model parameters	Correlation coefficient (r^2)	Adj. r^2	*p*-value	RMSE	AKB Model parameters	Correlation coefficient (r^2)	Adj. r^2	*p*-value	RMSE
Pseudo first order	20	$K_1 = 0.005$ $q_e = 2.14$	0.842	0.829	$3.68*10^{-6}$	0.155	$K_1 = 0.005$ $q_e = 2.15$	0.835	0.821	$4.86*10^{-6}$	0.161
	50	$K_1 = 0.005$ $q_e = 5.51$	0.647	0.618	$5.17*10^{-4}$	0.266	$K_1 = 0.009$ $q_e = 3.93$	0.949	0.944	$3.96*10^{-9}$	0.134
	100	$K_1 = 0.006$ $q_e = 4.90$	0.923	0.917	$4.50*10^{-8}$	0.121	$K_1 = 0.01$ $q_e = 5.32$	0.934	0.929	$1.79*10^{-8}$	0.156
	150	$K_1 = 0.005$ $q_e = 5.90$	0.903	0.895	$1.85*10^{-7}$	0.105	$K_1 = 0.012$ $q_e = 6.77$	0.937	0.932	$1.37*10^{-8}$	0.198
	200	$K_1 = 0.006$ $q_e = 6.53$	0.987	0.986	$8.76*10^{-13}$	0.046	$K_1 = 0.012$ $q_e = 7.76$	0.991	0.991	$7.16*10^{-13}$	0.059
Pseudo second order	20	$q_e = 12.65$ $K_2 = 0.0049$	0.997	0.997	$1.70*10^{-17}$	0.513	$q_e = 12.82$ $K_1 = 0.0043$	0.997	0.997	$1.70*10^{-17}$	0.513
	50	$q_e = 38.46$ $K_2 = 0.0029$	0.999	0.999	$7.72*10^{-20}$	0.109	$q_e = 43.47$ $K_1 = 0.0011$	0.997	0.994	$5.14*10^{-15}$	0.245
	100	$q_e = 71.42$ $K_2 = 0.00057$	0.997	0.996	$1.52*10^{-16}$	0.112	$q_e = 83.33$ $K_1 = 0.00056$	0.997	0.995	$1.24*10^{-16}$	0.098
	150	$q_e = 100$ $K_2 = 0.00034$	0.995	0.995	$1.87*10^{-15}$	0.102	$q_e = 111.11$ $K_1 = 0.00034$	0.995	0.995	$1.09*10^{-15}$	0.083
	200	$q_e = 100$ $K_2 = 0.00016$	0.975	0.973	$4.76*10^{-11}$	0.235	$q_e = 142.85$ $K_1 = 0.00014$	0.990	0.989	$2.14*10^{-13}$	0.108
Intraparticle diffusion	20	$K_{id} = 0.47$ $C = 4.405$	0.711	0.682	$5.66*10^{-4}$	0.883	$K_{id} = 0.47$ $C = 4.405$	0.660	0.626	$1.32*10^{-3}$	1.598
	50	$K_{id} = 1.38$ $C = 15.51$	0.692	0.661	$7.83*10^{-4}$	3.890	$K_{id} = 1.55$ $C = 14.55$	0.968	0.965	$7.31*10^{-9}$	1.186
	100	$K_{id} = 2.78$ $C = 17.75$	0.838	0.822	$2.89*10^{-5}$	6.081	$K_{id} = 3.11$ $C = 22.62$	0.899	0.889	$2.58*10^{-6}$	4.948
	150	$K_{id} = 3.88$ $C = 21.68$	0.980	0.978	$6.89*10^{-10}$	3.216	$K_{id} = 4.70$ $C = 24.80$	0.888	0.877	$4.51*10^{-6}$	8.410
	200	$K_{id} = 4.21$ $C = 8.12$	0.898	0.888	$2.74*10^{-6}$	6.544	$K_{id} = 6.01$ $C = 15.04$	0.928	0.921	$4.67*10^{-7}$	9.184
Elovich	20	$\beta = 0.48$ $\alpha = 2.85$	0.867	0.855	$3.74*10^{-6}$	0.898	$\beta = 0.48$ $\alpha = 2.85$	0.867	0.855	$3.74*10^{-6}$	0.898
	50	$\beta = 0.16$ $\alpha = 11.26$	0.860	0.847	$4.94*10^{-6}$	2.556	$\beta = 0.15$ $\alpha = 10.84$	0.979	0.977	$1.35*10^{-10}$	0.994
	100	$\beta = 0.08$ $\alpha = 9.71$	0.976	0.974	$2.67*10^{-10}$	2.342	$\beta = 0.07$ $\alpha = 13.68$	0.976	0.974	$2.76*10^{-10}$	2.405
	150	$\beta = 0.06$ $\alpha = 12.22$	0.968	0.965	$1.28*10^{-9}$	3.667	$\beta = 0.05$ $\alpha = 13.79$	0.982	0.980	$5.81*10^{-11}$	3.381
	200	$\beta = 0.06$ $\alpha = 6.59$	0.956	0.952	$7.56*10^{-9}$	5.018	$\beta = 0.04$ $\alpha = 9.92$	0.990	0.990	$1.42*10^{-12}$	3.312

AB: Algal Biochar, AKB: Algal Kombucha Biochar; MG: Malachite green.
k_1 – Pseudo-fisrt order Rate constant (min^{-1}); q_e – Amount of compound adsorbed at equilibrium (mg g^{-1}); k_2 – Pseudo-second order Rate constant (g mg^{-1} min^{-1}); α– Initial rate of biosorption (mg g^{-1} min^{-1}); β – !!!!!!!!!!Elovich constant (g mg^{-1}); Adj. r^2: Adjacent r^2; RMSE: Root mean square error.

this to occur in respective stages are: (1) MG diffused quickly from the bulk solution to the biochar surface (film diffusion), (2) MG particles diffused into pores of the biochar; however, they experienced diffusion resistance, resulting in a slower diffusion, and (3) MG further struggled to diffuse into the pores, and consequently, an equilibrium was established [39].

The datasets obtained in this study fitted well with both chemisorption and diffusion models; thus, both chemisorption and diffusion played essential roles in the rate-determining step. The combined diffusion-chemisorption model was a perfect fit for the lower concentrations of MG; however, when the concentration of MG started increasing (100–200 ppm), the R^2 value significantly decreased (from 0.99 to 0.65). This holds for both AB and AKB. Interestingly, the R^2 value for IPD plots increased (from 0.71 to 0.96) with the increasing concentration (20–200 ppm). These observations could have two possible inferences. First, chemisorption was not the rate-determining step when dealing with higher MG concentrations, and second, the diffusion became more and more significant (rate-determining) at higher MG concentrations. It might be because, in a lower concentration of MG, the particles interacted with the surface and were adsorbed through chemisorption. As the number of particles is low, the limited functional groups on the biochar surface can easily accommodate the particles making chemisorption the more dominating mechanism. However, the MG particles would quickly saturate the surface functional groups at a higher MG concentration. Hence, MG particles will try to slowly diffuse into the pores, making the diffusion process the dominant mechanism, as observed for MG adsorption onto chitosan beads [40].

In a nutshell, the adsorption of MG onto AB and AKB is a complex process that may involve several reactions, such as physical adsorption, electrostatic attraction, surface complex formation, and cation exchange reactions. The FTIR data indicates the presence of several functional groups on AB and AKB; these functional groups could adsorb MG molecules via surface complex formation, cation exchange reactions, or electrostatic interactions. Moreover, the adsorption of MG onto AB and AKB fits well with pseudo-second-order kinetics and with the Freundlich model. This indicates that the adsorption of MG on the AB and AKB could be controlled by several processes as discussed earlier. Moreover, depending on the chemical (abundance of functional groups) and physical (surface area and porosity) properties, the dominance of a process gets decided. For example, if the biochar has more abundant

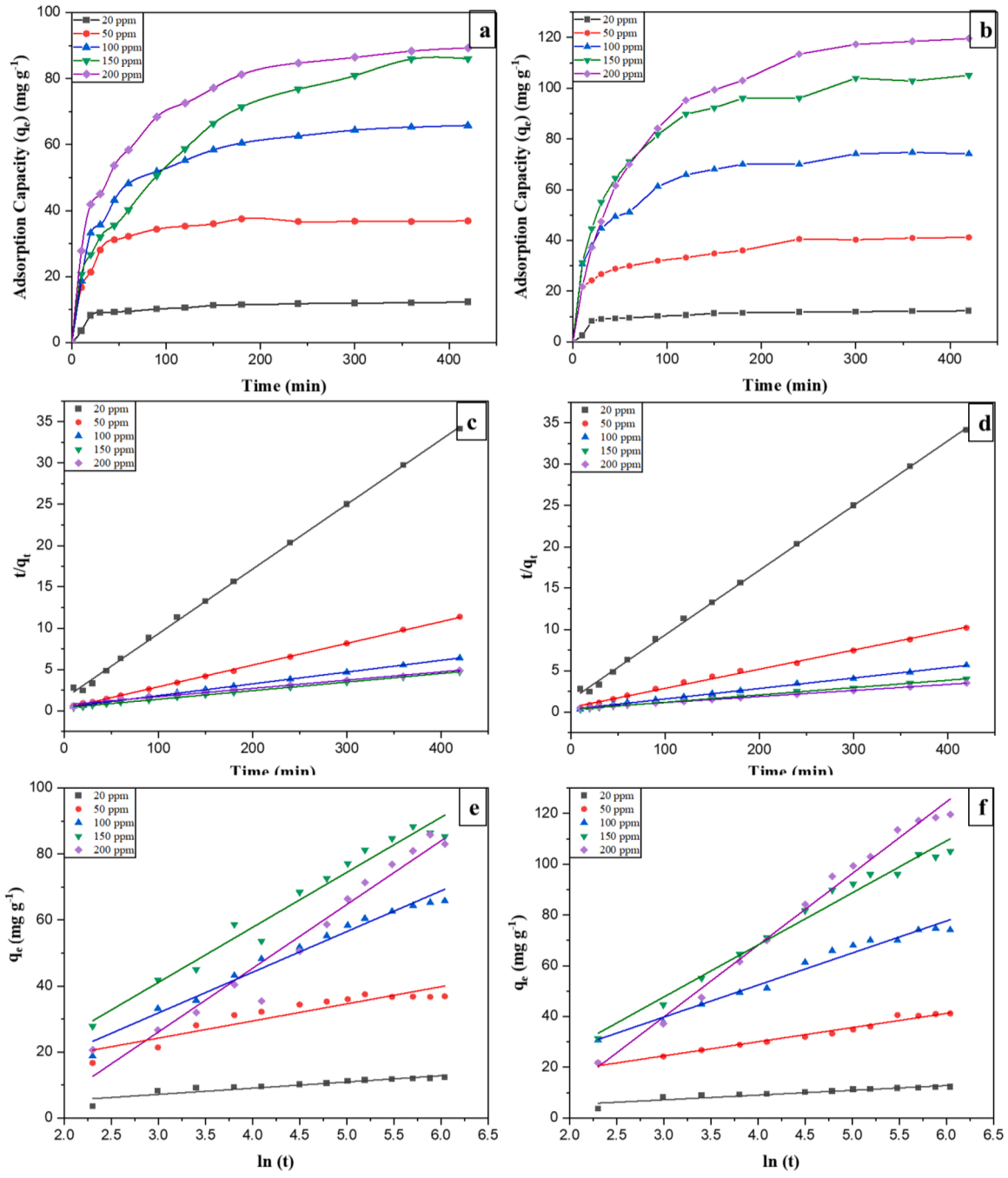

Fig. 3. Kinetic models fitted for malachite green adsorption by algal biochar and algal kombucha biochar. Kinetics plots (a) Algal biochar; (b) Algal kombucha biochar; Pseudo-second-order model (c) Algal biochar; (d) Algal kombucha biochar, and Elovich model (e) Algal biochar; (f) Algal kombucha biochar.
C_e: Equilibrium concentration of adsorbate (mg L^{-1}); q_e: Amount of compound adsorbed at equilibrium (mg g^{-1}); q_t: Amount of compound adsorbed at time "t" (mg g^{-1}); t: time (min).

functional groups, then chemical reactions (ion exchange, surface complex formation) could play a dominant role in the adsorption. Similarly, if the biochar has an appropriate porosity, it could accommodate a significant amount of MG molecules on its surface thus could act as a dominant mechanism of adsorption. Hence, as AB has more functional groups than AKB, chemisorption becomes dominant in adsorbing MG. However, after modification with kombucha SCOBY, the biochar surface properties improved, and thus physical adsorption also became a crucial mechanism in the adsorption process. Overall, algal biochar modified by SCOBY (AKB) exhibits better surface characteristics due to its inherent chemical properties (abundant functional groups from algae). This improves its removal efficiency by 10% and adsorption capacity from 166 to 500 mg g^{-1} (by almost three-fold).

3.5. Desorption of MG and reusability of biochars

For the desorption, both organic (alcohol-based chemicals) and inorganic (acids and alkali) dominated desorbent can be used. But, organic desorbent can be recycled and separated from the dye molecules *via* simple distillation [41]. Our desorption study indicates that for AB, the desorption of MG increased with increasing ethanol concentration (Fig. S6a). However, for AKB, the desorption of MG rose from 0 to 66% ethanol and then decreased from 66 to 100% ethanol (Fig. S6a). Hence, the proper eluent for MG desorption by AB and AKB is 100 and 66%

ethanol, respectively. The ethanol has both hydrophobic (–CH_2CH_3) and hydrophilic (–OH) functional groups; the hydrophobic group gets firmly attached to the aromatic structures of biochar, while the hydrophilic group interacts with surface functional groups (responsible for dye adsorption) such as –OH, –COOH present on the biochar surface. Therefore, the ethanol competes with MG molecules for the adsorption sites, displacing them from the surface and blocking their biochar interaction [41]. MG molecules are better soluble in water than ethanol, so water in the desorbing solvent could help stabilize the desorbed MG particles from the surface and prevent their re-interaction with the biochar. This could explain the highest desorption at 66% of ethanol concentration for AKB.

The adsorption efficiency for five consecutive cycles for AB and AKB was decreased slightly from 84 to 81% and from 88 to 84.5%, respectively (Fig. S6b). The slight decreases in the adsorption efficiency might be due to the loss of active adsorption sites and blockage of biochar surface pores [42]. The regeneration study shows a comparatively small (less than 4%) reduction in removal efficiency over successive cycles. The biochar still had more than 80% efficiency, suggesting that the prepared adsorbent was highly reusable.

Some of the critical future challenges could be associated with the prepared adsorbent. The adsorbents were prepared from a microalgae consortium (a group of microalgae). Thus its chemical properties might vary based on the dominant algal groups in the consortium. Synthesizing composite with SCOBY could be impacted by the availability of kombucha SCOBY. Hence, it becomes crucial to produce the desired amount of SCOBY to scale up the production of the adsorbent. Another critical challenge could be the disposal of the spent adsorbent, and a potential method is to use the spent biochar in land fills or as soil amendments. Moreover, recent research shows that biochar could be used as a construction material [43]. Thus the spent adsorbent (biochar) could be a cheaper source for the applications discussed above.

The cost of reusing the biochar is primarily affected by two aspects: (1) the cost of the desorbent, and (2) the cost of drying the biochar. The cost of desorbent is not that high as compared to the production cost of biochar. The latter includes: (1) cultivating algae, (2) harvesting algae, (3) pyrolysis of harvested algae. The cultivation and harvesting of the algae was estimated to be around 110–670 USD t^{-1} [44], whereas production of biochar will cost an additional 350–1200 USD t^{-1} [45]. Thus, it seems quite economical to reuse the biochar after desorption.

3.6. *Integrating phycoremediation to biochar remediated water enhanced the MG removal and algal growth*

Phycoremediation was integrated with biosorption to attain maximum efficiency and reuse the remediated water for microalgal cultivation. This integration can also help in achieving a trade-off between cost and time factors, as biosorption and phycoremediation are individually chemical-intensive and time-consuming processes. It is worth noting that both living and nonliving algal biomass can be utilized to remediate dyes from aqueous solutions. It is seen in literature that the remediation time lies in between 5 and 14 days depending upon the

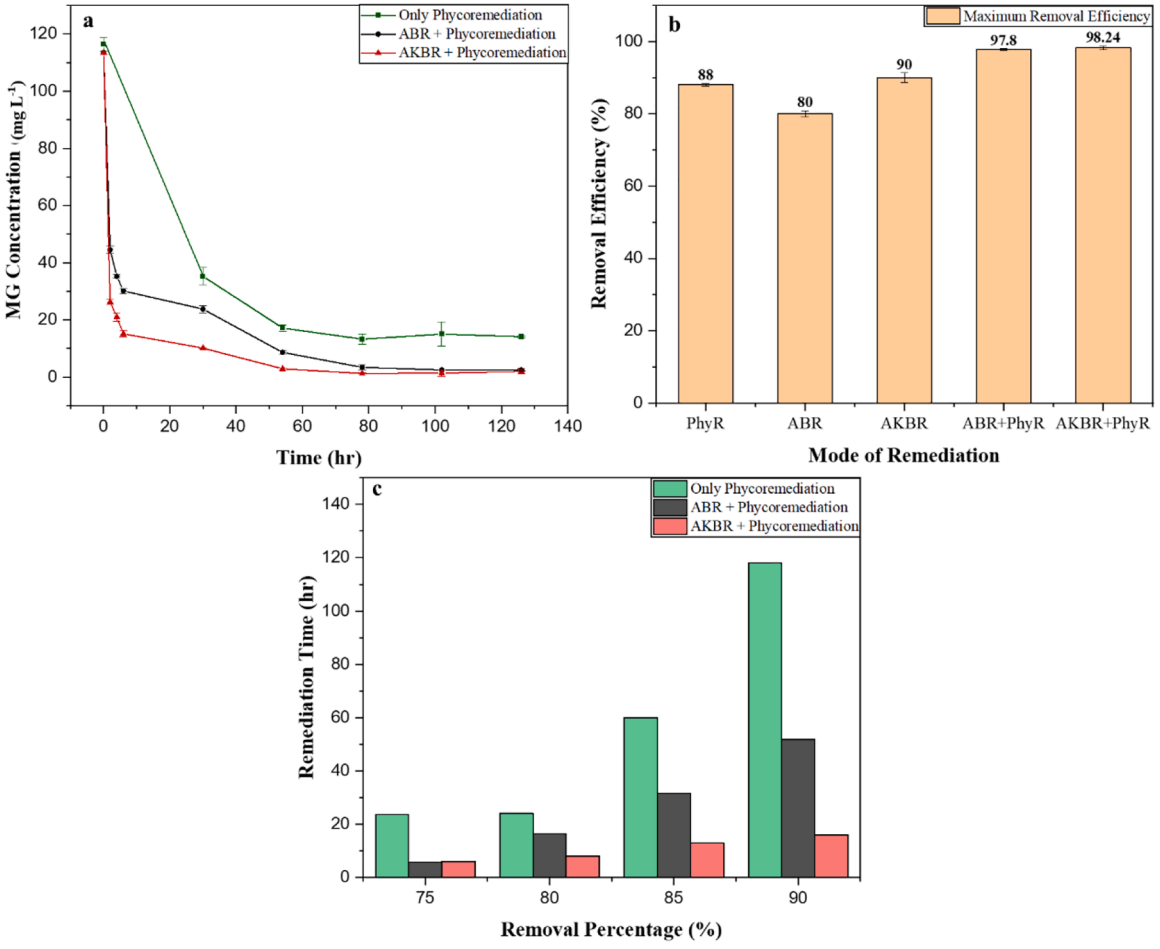

Fig. 4. Phycoremediation experiments: (a) Removal of malachite green from the solution for only phycoremediation and via integrated adsorption- phycoremediation; (b) Time taken by different processes to achieve the desired removal efficiency; (c) Maximum removal efficiency achieved through an individual/integrated process.
ABR: Algal biochar remediated, AKBR: Algal kombucha biochar remediated, MG: Malachite green, AB: Algal biochar, AKB: Algal kombucha biochar

Table 3
Algal growth and productivity achieved through the integrated process.

	BG11 + fresh water	BG11 + MG solution	BG11 + AB remediated water	BG11 + AKB remediated water
Initial amount of MG present (ppm)	0	100	23	10
pH	6.5-7.0	4.00	6.7-7.5	6.8-7.3
Weight of the harvested algae (mg L^{-1})	546	50	720	840
Algal productivity (mg L^{-1} day^{-1})	47.4	2.3	63.3	74.0
Increase in algal growth (%)*	0	-95	33	55

AB: Algal Biochar, AKB: Algal-Kombucha Biochar, MG: Malachite green, BG-11: Nutrient media used for algal cultivation
* as compared to normal condition.

types of dyes and its initial concentration in the solution; yet, leading to complete adsorption or biotransformation of the dyes [46–48].

In this study, live algal biomass was used to remediate the remaining MG. The removal rate of MG significantly improved with integration, making the overall process effective **(**Fig. 4**a).** It can be observed from Fig. 4b that the time required to achieve the desired efficiency is considerably higher for phycoremediation than the integrated process. When desorption of MG removed by algae was performed using ethanol, no leaching of MG into the solution was observed. This confirms that the mechanism opted by algae for remediation was biotransformation instead of adsorption. It is reported that the living algal cells can degrade the dyes by the activities of enzymes such as laccase, polyphenol oxidase, and azo reductase [47,49].

If we study the processes individually, the maximum efficiencies achieved with adsorption using AB and AKB and phycoremediation were 82%, 90%, and 88%, respectively. However, when adsorption was integrated with phycoremediation, the maximum removal efficiency reached 98% (Fig. 4c). The reason could be related to the use of living algal cells for remediating MG. It is recorded in previous studies that a higher dye concentration (more than 50 mg L^{-1}) impedes algal growth, consequently affecting the removal efficiency. However, phycoremediation *via* living algae becomes faster and efficient at low dye concentrations (0–50 mg L^{-1}) [50]. After adsorption using biochar, the MG concentration in the remediated water reduced from 100 mg L^{-1} to 10–20 mg L^{-1}. Hence, it can be combined with phycoremediation to remediate the pollutants completely. Algae grown in the AKB remediated wastewater had the highest growth, followed by AB remediated wastewater, distilled water, and concentrated MG solution (Table 3). Moreover, microalgal growth was increased by 1.33 and 1.55 times in the AB and AKB remediated water, respectively, than in freshwater. The enhanced algal growth in AB and AKB remediated water could be primarily due to the following two reasons. Firstly, the pH of the solution plays a crucial role in algal growth. Algae requires neutral or slightly alkaline pH for their growth; but the pH of malachite green is acidic (around 3.5–4) in nature. This might have hindered the algal growth in concentrated MG solution [46].

On the other hand, the pH of the prepared biochar was measured to be in the range of 6.5–7.5. Thus, when the biochar was added to the MG solution, it could increase the pH to a suitable range for algal growth (for instance, from neutral to slightly basic pH). Secondly, leaching of inorganic nutrients from biochar into the solution could contribute to algal growth. Apart from carbon dioxide, microalgae require nitrogen and phosphorus for their growth; hence, the growth could be stimulated in the presence of N and P [51]. Algal biochar has a higher nitrogen content than biochar prepared from other biomasses, [52], which might have supported the algal growth in the remediated water. Moreover, the elemental analysis confirmed the presence of inorganic nutrients such as P, Mg that could be beneficial for algal growth (Table S3). Algal biochar could leach some inorganic nutrients to the solution. Thus, the presence of inorganic nutrients in AB and AKB remediated water (compared to BG-11 media prepared with distilled water) might have enhanced the algal growth.

The integration of adsorption and phycoremediation processes complement each other by overcoming cost and time limitations concerning each process. Phycoremediation is not suitable for remediating higher concentrations of MG, but it is quite effective at a lower concentration. On the other hand, adsorption is effective in higher concentrations but cannot completely eliminate the pollutants (the pollutants remain in the environment). However, when the living algal cells were utilized for the phycoremediation, the MG was degraded completely. The algae regenerated from the phycoremediation can be used in various applications, including preparing the biochar and rendering the integrated adsorption-phycoremediation processes circular. Hence, this integrated model for remediation can be extended to other dyes and pollutants in the future.

4. Conclusion

Chemisorption was the dominant mechanism in removing MG when its concentration was low, whereas diffusion became prevalent at a higher concentration of MG when biochar was used to remediate MG-contaminated wastewater. Higher algal growth in remediated water and excellent removal efficiency highlights the advantage of integrating the adsorption-phycoremediation processes. The integration of processes would help utilize economical and environment-friendly adsorbents for remediating pollutants sustainably. Future studies should focus on the applicability of this integrated remediation system for other contaminants to make the overall process more aligned towards a circular economy.

Supplementary data

E-supplementary data for this work can be found in online version of the paper.

CRediT authorship contribution statement

Abhijeet Pathy: Conceptualization, Visualization, Methodology, Formal analysis, Writing – original draft. **Nageshwari Krishnamoorthy:** Methodology, Writing – original draft. **Scott X. Chang:** Supervision, Investigation, Writing – review & editing. **Balasubramanian Paramasivan:** Conceptualization, Supervision, Funding acquisition, Writing – review & editing.

Declaration of Competing Interest

The authors declare that they have no known competing financial interests or personal relationships that could have appeared to influence the work reported in this paper.

Acknowledgments

The authors thank the Department of Biotechnology and Medical Engineering of the National Institute of Technology Rourkela for providing the research facility. The authors greatly acknowledge the Ministry of Science and Technology of the Government of India for sponsoring the Ph.D. programme of the second author through ASEAN - India Science, Technology & Innovation Cooperation [File No. IMRC/

AISTDF/CRD/2018/000082]. The corresponding author acknowledge the Department of Biotechnology (DBT) of Government of India for funding the research under Biotechnology Ignition Grant (BIG) of Biotechnology Industry Research Assistance Council (BIRAC) *[BIRAC/KIIT0471/BIG-13/18]*.

Supplementary materials

Supplementary material associated with this article can be found, in the online version, at doi:10.1016/j.surfin.2022.101880.

References

[1] Y. Zhang, W. Yu, L. Pei, K. Lai, B.A. Rasco, Y. Huang, Rapid analysis of malachite green and leucomalachite green in fish muscles with surface-enhanced resonance Raman scattering, Food Chem. 169 (2015) 80–84, https://doi.org/10.1016/j.foodchem.2014.07.129.

[2] M.A. Khan, M. Otero, M. Kazi, A.A. Alqadami, S.M. Wabaidur, M.R. Siddiqui, S. Sumbul, Unary and binary adsorption studies of lead and malachite green onto a nanomagnetic copper ferrite/drumstick pod biomass composite, J. Hazard. Mater. 365 (2019) 759–770, https://doi.org/10.1016/j.jhazmat.2018.11.072.

[3] S. Srivastava, R. Sinha, D. Roy, Toxicological effects of malachite green, Aquat. Toxicol. 66 (3) (2004) 319–329, https://doi.org/10.1016/j.aquatox.2003.09.008.

[4] D. Shukla, M. Das, D. Kasade, M. Pandey, A.K. Dubey, S.K. Yadav, A.S. Parmar, Sandalwood-derived carbon quantum dots as bioimaging tools to investigate the toxicological effects of malachite green in model organisms, Chemosphere 248 (2020), 125998, https://doi.org/10.1016/j.chemosphere.2020.125998.

[5] J.K. Park, E.J. Rupa, M.H. Arif, J.F. Li, G. Anandapadmanaban, J.P. Kang, S. C. Kang, Synthesis of zinc oxide nanoparticles from Gynostemma pentaphyllum extracts and assessment of photocatalytic properties through malachite green dye decolorization under UV illumination-a green approach, Optik 239 (2021), 166249, https://doi.org/10.1016/j.ijleo.2020.166249.

[6] P. Chaijak, Malachite green removal and bio-electricity generation using a novel-design multi-electrode microbial fuel cell, Acta Sci. Pol. Form. Circumiectus 20 (1) (2021) 69–76, https://doi.org/10.15576/ASP.FC/2021.20.1.69.

[7] D. Ghime, P. Ghosh, Advanced oxidation processes: a powerful treatment option for the removal of recalcitrant organic compounds, in: Ciro Bustillo-Lecompte (Ed.), Advanced Oxidation Processes-Applications, Trends, and Prospects, IntechOpen, 2020, pp. 3–14.

[8] Q. Ren, C. Kong, Z. Chen, J. Zhou, W. Li, D. Li, Y. Lu, Ultrasonic assisted electrochemical degradation of malachite green in wastewater, Microchem. J. 164 (2021), 106059, https://doi.org/10.1016/j.microc.2021.106059.

[9] M. Hijab, J. Saleem, P. Parthasarathy, H.R. Mackey, G. McKay, Two-stage optimisation for malachite green removal using activated date pits, Biomass Convers. Biorefin. 11 (2) (2021) 727–740, https://doi.org/10.1007/s13399-020-00813-y.

[10] S. Rangabhashiyam, S. Lata, P. Balasubramanian, Biosorption characteristics of methylene blue and malachite green from simulated wastewater onto Carica papaya wood biosorbent, Surf. Interfaces 10 (2018) 197–215, https://doi.org/10.1016/j.surfin.2017.09.011.

[11] S. Rangabhashiyam, N. Anu, M.S. Giri Nandagopal, N. Selvaraju, Relevance of isotherm models in biosorption of pollutants by agricultural byproducts, J. Environ. Chem. Eng. 2 (1) (2014) 398–414, https://doi.org/10.1016/j.jece.2014.01.014.

[12] M.J. Ahmed, B.H. Hameed, E.H. Hummadi, Review on recent progress in chitosan/chitin-carbonaceous material composites for the adsorption of water pollutants, Carbohydr. Polym. 247 (2020), 116690, https://doi.org/10.1016/j.carbpol.2020.116690.

[13] K. Tewari, G. Singhal, R.K. Arya, Adsorption removal of malachite green dye from aqueous solution, Rev. Chem. Eng. 34 (3) (2018) 427–453, https://doi.org/10.1515/revce-2016-0041.

[14] A. Pathy, J. Ray, B. Paramasivan, Challenges and opportunities of nutrient recovery from human urine using biochar for fertilizer applications, J. Clean. Prod. 304 (2021), 127019, https://doi.org/10.1016/j.jclepro.2021.127019.

[15] I. Kozyatnyk, P. Oesterle, C. Wurzer, O. Mašek, S. Jansson, Removal of contaminants of emerging concern from multicomponent systems using carbon dioxide activated biochar from lignocellulosic feedstocks, Bioresour. Technol. 340 (2021), 125561, https://doi.org/10.1016/j.biortech.2021.125561.

[16] H.L. Bryant, I. Gogichaishvili, D. Anderson, J.W. Richardson, J. Sawyer, T. Wickersham, M.L. Drewery, The value of post-extracted algae residue, Algal Res. 1 (2) (2012) 185–193, https://doi.org/10.1016/j.algal.2012.06.001.

[17] K.L. Yu, B.F. Lau, P.L. Show, H.C. Ong, T.C. Ling, W.H. Chen, J.S. Chang, Recent developments on algal biochar production and characterization, Bioresour. Technol. 246 (2017) 2–11, https://doi.org/10.1016/j.biortech.2017.08.009, 2017.

[18] E. Fosso-Kankeu, J. Potgieter, F.B. Waanders, Removal of malachite green and toluidine blue dyes from aqueous solution using a clay-biochar composite of bentonite and sweet sorghum bagasse, Int. J. Appl. Eng. Res. 14 (6) (2019) 1324–1333. http://hdl.handle.net/10394/34291.

[19] M. Zubair, I. Ihsanullah, H. Abdul Aziz, M. Azmier Ahmad, M.A. Al-Harthi, Sustainable wastewater treatment by biochar/layered double hydroxide composites: Progress, challenges, and outlook, Bioresour. Technol. 319 (2020), 124128, https://doi.org/10.1016/j.biortech.2020.124128.

[20] J. Song, S.A. Messele, L. Meng, Z. Huang, M.G. El-Din, Adsorption of metals from oil sands process water (OSPW) under natural pH by sludge-based biochar/chitosan composite, Water Res. 194 (2021), 116930, https://doi.org/10.1016/j.watres.2021.116930.

[21] D. Laavanya, S. Shirkole, P. Balasubramanian, Current challenges, applications and future perspectives of SCOBY cellulose of kombucha fermentation, J. Clean. Prod. 295 (2021), 126454, https://doi.org/10.1016/j.jclepro.2021.126454.

[22] Y. Dai, N. Zhang, C. Xing, Q. Cui, Q. Sun, The adsorption, regeneration and engineering applications of biochar for removal organic pollutants: a review, Chemosphere 223 (2019) 12–27, https://doi.org/10.1016/j.chemosphere.2019.01.161.

[23] V.V. Priyan, T. Shahnaz, E. Suganya, S. Sivaprakasam, S. Narayanasamy, Ecotoxicological assessment of micropollutant diclofenac biosorption on magnetic sawdust: phyto, microbial and fish toxicity studies, J. Hazard. Mater. 403 (2021), 123532, https://doi.org/10.1016/j.jhazmat.2020.123532.

[24] B. Behera, M. Selvam S, B. Dey, P. Balasubramanian, Algal biodiesel production with engineered biochar as a heterogeneous solid acid catalyst, Bioresour. Technol. 310 (2020), 123392, https://doi.org/10.1016/j.biortech.2020.123392.

[25] R. Jayabalan, R.V Malbaša, E.S. Lončar, J.S. Vitas, M. Sathishkumar, A review on kombucha tea—microbiology, composition, fermentation, beneficial effects, toxicity, and tea fungus, Comprehensive Reviews in Food Science and Food Safety 13 (4) (2014) 538–550, https://doi.org/10.1111/1541-4337.12073.

[26] H. Li, X. Dong, E.B. da Silva, L.M. de Oliveira, Y. Chen, L.Q. Ma, Mechanisms of metal sorption by biochars: biochar characteristics and modifications, Chemosphere 178 (2017) 466–478, https://doi.org/10.1016/j.chemosphere.2017.03.072.

[27] H. Omar, A. El-Gendy, K. Al-Ahmary, Bioremoval of toxic dye by using different marine macroalgae, Turk. J. Bot. 42 (1) (2018) 15–27, https://doi.org/10.3906/bot-1703-4.

[28] P. Nautiyal, K.A. Subramanian, M.G. Dastidar, Adsorptive removal of dye using biochar derived from residual algae after *in-situ* transesterification: alternate use of waste of biodiesel industry, J. Environ. Manag. 182 (2016) 187–197, https://doi.org/10.1016/j.jenvman.2016.07.063.

[29] K. Kalaiappan, S. Marimuthu, S. Rengapillai, R. Murugan, T Premkumar, Kombucha SCOBY-based carbon as a green scaffold for high-capacity cathode in lithium–sulfur batteries, Ionics 25 (10) (2019) 4637–4650, https://doi.org/10.1007/S11581-019-03018-0 (Kiel).

[30] A. Tomczyk, Z. Sokołowska, P. Boguta, Biochar physicochemical properties: pyrolysis temperature and feedstock kind effects, Rev. Environ. Sci. Biotechnol. 19 (1) (2020) 191–215, https://doi.org/10.1007/S11157-020-09523-3.

[31] R. Malik, D.S. Ramteke, S.R. Wate, Adsorption of malachite green on groundnut shell waste based powdered activated carbon, Waste Manag. 27 (9) (2007) 1129–1138, https://doi.org/10.1016/j.wasman.2006.06.009.

[32] S. Chowdhury, R. Mishra, P. Saha, P. Kushwaha, Adsorption thermodynamics, kinetics and isosteric heat of adsorption of malachite green onto chemically modified rice husk, Desalination 265 (1–3) (2011) 159–168, https://doi.org/10.1016/j.desal.2010.07.047.

[33] E.R. García, R.L. Medina, M.M. Lozano, I.H. Pérez, M.J. Valero, A.M. Maubert Franco, Adsorption of azo-dye orange II from aqueous solutions using a metal-organic framework material: iron- benzenetricarboxylate, Materials 7 (12) (2014) 8037–8057, https://doi.org/10.3390/MA7128037.

[34] E. Boorboor Azimi, A. Badiei, J.B. Ghasemi, Efficient removal of malachite green from wastewater by using boron-doped mesoporous carbon nitride, Appl. Surf. Sci. 469 (2019) 236–245, https://doi.org/10.1016/j.apsusc.2018.11.017.

[35] S. Rangabhashiyam, P. Balasubramanian, Performance of novel biosorbents prepared using native and NaOH treated Peltophorum pterocarpum fruit shells for the removal of malachite green, Bioresour. Technol. Rep. 3 (2018) 75–81, https://doi.org/10.1016/j.biteb.2018.06.004, 2018.

[36] N. Ayawei, S.S. Angaye, D. Wankasi, E.D. Dikio, Synthesis, characterization and application of Mg/Al layered double hydroxide for the degradation of congo red in aqueous solution, Open J. Phys. Chem. 05 (03) (2015) 56–70, https://doi.org/10.4236/OJPC.2015.53007.

[37] S. Fan, Y. Wang, Y. Li, J. Tang, Z. Wang, J. Tang, K Hu, Facile synthesis of tea waste/Fe_3O_4 nanoparticle composite for hexavalent chromium removal from aqueous solution, RSC Adv. 7 (13) (2017) 7576–7590, https://doi.org/10.1039/c6ra27781k.

[38] Y. Zhou, X. Liu, Y. Xiang, P. Wang, J. Zhang, F. Zhang, L. Tang, Modification of biochar derived from sawdust and its application in removal of tetracycline and copper from aqueous solution: adsorption mechanism and modelling, Bioresour. Technol. 245 (2017) 266–273, https://doi.org/10.1016/j.biortech.2017.08.178.

[39] A.S. Eltaweil, H. Ali Mohamed, E.M. Abd El-Monaem, G.M. El-Subruiti, Mesoporous magnetic biochar composite for enhanced adsorption of malachite green dye: characterization, adsorption kinetics, thermodynamics and isotherms, Adv. Powder Technol. 31 (3) (2020) 1253–1263, https://doi.org/10.1016/j.apt.2020.01.005.

[40] Z. Bekçi, C. Özveri, Y. Seki, K. Yurdakoç, Sorption of malachite green on chitosan bead, J. Hazard. Mater. 54 (1–3) (2008) 254–261, https://doi.org/10.1016/j.jhazmat.2007.10.021.

[41] X. Xing, H. Qu, R. Shao, Q. Wang, H. Xie, Mechanism and kinetics of dye desorption from dye-loaded carbon (XC-72) with alcohol-water system as desorbent, Water Sci. Technol. 76 (5) (2017) 1243–1250, https://doi.org/10.2166/wst.2017.268.

[42] M. Choudhary, R. Kumar, S. Neogi, Activated biochar derived from Opuntia ficus-indica for the efficient adsorption of malachite green dye, Cu^{+2} and Ni^{+2} from water, J. Hazard. Mater. 392 (2020), 122441, https://doi.org/10.1016/j.jhazmat.2020.122441.

[43] S. Gupta, Kua H.W., Factors determining the potential of biochar as a carbon capturing and sequestering construction material: critical review, *Journal of Materials in Civil Engineering*, 29(9) (2017) 04017086, doi: 10.1061/(asce)mt.1943-5533.0001924.

[44] F. Fasaei, J.H. Bitter, P.M. Slegers, A.J.B. van Boxtel, Techno-economic evaluation of microalgae harvesting and dewatering systems, Algal Res. 31 (2017) 347–362, https://doi.org/10.1016/j.algal.2017.11.038.

[45] K.A. Thompson, K.K. Shimabuku, J.P. Kearns, D.R.U. Knappe, R.S. Summers, S. M. Cook, Environmental comparison of biochar and activated carbon for tertiary wastewater treatment, Environ. Sci. Technol. 50 (20) (2016) 11253–11262, https://doi.org/10.1021/acs.est.6b03239.

[46] G. Boduroğlu, N.K. Kiliç, G. Dönmez, Bioremoval of reactive blue 220 by gonium sp. biomass, Environ. Technol. 35 (19) (2014) 2410–2415, https://doi.org/10.1080/09593330.2014.908240.

[47] B. Priya, L. Uma, A.K. Ahamed, G. Subramanian, D. Prabaharan, Ability to use the diazo dye, CI acid black 1 as a nitrogen source by the marine cyanobacterium Oscillatoria curviceps BDU92191, Bioresour. Technol. 102 (14) (2011) 7218–7223, https://doi.org/10.1016/j.biortech.2011.02.117.

[48] M.M. El-Sheekh, M.M. Gharieb, G.W. Abou-El-Souod, Biodegradation of dyes by some green algae and cyanobacteria, Int. Biodeterior. Biodegrad. 63 (6) (2009) 699–704, https://doi.org/10.1016/j.ibiod.2009.04.010.

[49] S.K. Saha, P. Swaminathan, C. Raghavan, L. Uma, G. Subramanian, Ligninolytic and antioxidative enzymes of a marine cyanobacterium Oscillatoria willei BDU 130511 during poly R-478 decolourization, Bioresour. Technol. 101 (9) (2010) 3076–3084, 101(9) (2010) 3076-3084.

[50] G.G. Gelebo, L.H. Tessema, K.T. Kehshin, H.H. Gebremariam, E.T. Gebremikal, M. T. Motuma, A. Suresh, Phycoremediation of synthetic dyes in an aqueous solution using an indigenous Oscillatoria sp., from Ethiopia, Ethiop. J. Sci. Sustain. Dev. 7 (2) (2020) 14–20, https://doi.org/10.20372/ejssdastu.

[51] D. Kaplan, A.E. Richmond, Z. Dubinsky, S. Aaronson, Algal nutrition, Cell response to environmental factors, in: A Richmond (Ed.), CRC Handbook of Microalgal Mass Culture, CRC Press, 2017, pp. 69–100.

[52] A. Pathy, S. Meher, P. Balasubramanian, Predicting algal biochar yield using eXtreme Gradient Boosting (XGB) algorithm of machine learning methods, Algal Res. 50 (2020), 102006, https://doi.org/10.1016/j.algal.2020.102006.